

Passivity Enforcement for Transmission Line Models Based on the Method of Characteristics

Bjørn Gustavsen, *Senior Member, IEEE*

Abstract—The Universal Line Model (ULM) has been implemented in several EMT programs for simulation of electromagnetic transients. In some cases, instability problems have been encountered. This paper shows that the current approach for rational function approximation adopted in ULM can lead to large out-of-band passivity violations, thereby causing an unstable simulation. An approach is introduced which prevents the occurrence of large passivity violations. Low-frequency violations are avoided by adding an artificial shunt conductance to the diagonal elements of the shunt admittance matrix while high-frequency violations are avoided by introducing artificial attenuation using a low-pass filter. In addition, high-frequency asymptotic passivity is enforced for the characteristic admittance. Any remaining violations are removed by adding a second-order correction term to the model ports. The approach is shown to mitigate instabilities from a cable system transient simulation, without impairing the quality of the model.

Index Terms—Electromagnetic transients, instability, passivity, transmission line model, universal line model.

I. INTRODUCTION

FREQUENCY-DEPENDENT transmission line models are widely applied in electromagnetic transients programs. These models are usually based on the Method of Characteristics (traveling wave method) with rational approximation of the propagation function and the characteristic impedance, leading to recursive convolution in the time domain [1]. While the early line models were based on a constant transformation matrix and modes [1], [2], several new line models have been proposed that are based on a formulation in phase co-ordinates [3]–[9]. Since no assumption of a constant transformation matrix is made, more accurate results can in general be achieved.

One of the phase domain models, the so-called Universal Line Model (ULM) [8], [9], is based on obtaining poles and delays via mode fitting, while calculating the final residues in the phase domain. Although highly successful in most situations, some deficiencies have become apparent. Some cable cases have been encountered where mode fitting will not produce suitable poles and delays. This problem was overcome in [10] by introduction of trace fitting. A more serious problem is that the ULM sometimes gives an unstable simulation result.

Manuscript received July 6, 2007; revised September 2, 2007. Current version published September 24, 2008. This work was supported by the Norwegian Research Council (PETROMAKS Programme) and by Deutsch, FMC Technologies, Framo, Norsk Hydro, Siemens, Statoil, Total, and Vetco Gray. Paper no. TPWRD-00380-2007.

The author is with SINTEF Energy Research, N-7465 Trondheim, Norway (e-mail: bjorn.gustavsen@sintef.no).

Digital Object Identifier 10.1109/TPWRD.2008.919034

This paper shows that the ULM formulation can easily lead to large out-of-band passivity violations and thus an unstable simulation. A practical approach is introduced which prevents the occurrence of out-of-band passivity violations, and a remedy is provided for removing any remaining in-band violations. Application to a cable case is shown to mitigate an unstable simulation.

In the examples, the calculation of per-unit-length cable parameters and the rational modeling is done using Matlab codes. The resulting model parameters are exported to the PSCAD simulation environment [11] and used within the existing ULM implementation (phase domain line).

II. UNIVERSAL LINE MODEL

A. Method of Characteristics in the Phase Domain

For a homogenous transmission line with ends k and m , the relation between voltage \mathbf{v} and current \mathbf{i} at end k is in the frequency domain given by the matrix-vector relations

$$\mathbf{i}_k = \mathbf{Y}_c \mathbf{v}_k - 2\mathbf{i}_{ki} \quad (1)$$

$$\mathbf{i}_{ki} = \mathbf{H}^T \mathbf{i}_{mr} \quad (2)$$

where indices i and r respectively denote incident and reflected wave. For a line of length l , the matrices for surge admittance \mathbf{Y}_c and propagation function \mathbf{H} are obtained from the series impedance \mathbf{Z} and shunt admittance \mathbf{Y} as

$$\mathbf{Y}_c = \mathbf{Z}^{-1} \sqrt{\mathbf{Z}\mathbf{Y}} \quad (3)$$

$$\mathbf{H} = e^{-\sqrt{\mathbf{Z}\mathbf{Y}}l} \quad (4)$$

B. Rational Fitting

In the Universal Line Model (ULM) [8] as implemented in PSCAD [9], the poles for \mathbf{Y}_c are obtained by fitting the matrix trace (5) using vector fitting (VF) [12], followed by a final fitting of the residues \mathbf{R}_m and proportional term \mathbf{D} in the phase domain (6). The fitting can also be done by applying VF to the columns of \mathbf{Y}_c as in the original formulation [8], giving a private pole set for each column

$$\text{tr}(\mathbf{Y}_c) = \sum_i \mathbf{Y}_{ii} \cong \sum_{m=1}^N \frac{r_m}{s - a_m} + d \quad (5)$$

$$\mathbf{Y}_c \cong \sum_{m=1}^N \frac{\mathbf{R}_m}{s - a_m} + \mathbf{D} \quad (6)$$

Poles and delays for the fitting of \mathbf{H} are obtained by fitting the modes h_i of \mathbf{H}

$$h_i \cong \sum_{m=1}^{N_i} \frac{r_{m,i}}{s - a_{m,i}} e^{-s\tau_i}, \quad i = 1, \dots, n. \quad (7)$$

Modes with nearly equal delays are lumped before doing the fitting. Finally, the residues $\{\mathbf{R}_m\}$ are calculated by solving (8) with (known) poles and delays obtained from the modes

$$\mathbf{H} \cong \sum_{g=1}^G \left(\sum_{m=1}^{N_g} \frac{\mathbf{R}_{m,g}}{s - a_{m,g}} \right) e^{-s\tau_g}. \quad (8)$$

In (8), G denotes the number of (lumped) modes and N_g is the number of poles used for fitting the g th mode.

It is also possible to extract the poles by fitting the matrix trace of \mathbf{H} , as suggested in [10]

$$\text{tr}(\mathbf{H}(s)) = \sum_i \mathbf{H}_{ii}(s). \quad (9)$$

III. PASSIVITY

The fitting of modes (or trace) and subsequent phase domain fitting of \mathbf{H} and \mathbf{Y}_c is done within a user-defined band. Although the fitting process ensures a high accuracy model within the band, there is no guarantee that the model behavior is acceptable outside this band. It will be shown that inaccurate out-of-band behavior can lead to large passivity violations and thus unstable simulations.

The fitting errors of \mathbf{H} and \mathbf{Y}_c result in the nodal admittance matrix \mathbf{Y}_n becoming slightly unsymmetrical. Passivity of an unsymmetrical model entails that \mathbf{Y}_H in (10) has all of its eigenvalue positive [13] where superscript H denotes Hermitian (transpose and conjugate). \mathbf{Y}_H has all of its eigenvalues real

$$\text{eig}(\mathbf{Y}_H) = \text{eig}((\mathbf{Y}_n(s) + \mathbf{Y}_n^H(s))/2) > 0 \quad \forall s, \quad s = j\omega. \quad (10)$$

The admittance matrix can be calculated directly from the rational approximations for \mathbf{H} and \mathbf{Y}_c as follows [15]

$$\mathbf{Y}_n = \begin{bmatrix} \mathbf{A} & \mathbf{B} \\ \mathbf{B} & \mathbf{A} \end{bmatrix} \quad (11)$$

where

$$\mathbf{A} = \mathbf{Y}_c(\mathbf{I} + \mathbf{H}^2)(\mathbf{I} - \mathbf{H}^2)^{-1} \quad (12)$$

$$\mathbf{B} = -2\mathbf{Y}_c\mathbf{H}(\mathbf{I} - \mathbf{H}^2)^{-1}. \quad (13)$$

Algebraic tests for passivity checking of transmission line models are discussed in [16].

IV. AVOIDING OUT-OF BAND PASSIVITY VIOLATIONS

A. Low-Frequency Passivity Violations

The magnitude of \mathbf{Y}_c approaches zero at DC when the shunt admittance \mathbf{Y} is purely capacitive, $\mathbf{Y} = s\mathbf{C}$. However, when calculating a rational approximation of \mathbf{Y}_c within a finite frequency band, a nonzero dc response will result. With the early

frequency dependent line models, it was found that this uncontrolled behavior near dc may lead to simulation instabilities [17]. As a practical remedy, it was proposed to insert an artificial shunt conductance to obtain a nonzero \mathbf{Y}_c at dc, an approach that has been adopted by several EMT programs [18]. A recent discussion can be found in [19]. Values for the shunt conductance that can occur in actual overhead line systems are discussed in [20].

Adding a conductance \mathbf{G}_{ii} to the diagonal elements of \mathbf{G} (14) causes $\mathbf{Y}_{c,ii}$ to approach a nonzero value (15) while \mathbf{H}_{ii} approaches a value smaller than unity (16)

$$\mathbf{Y}_{ii} = \mathbf{G}_{ii} + s\mathbf{C}_{ii} \quad (14)$$

$$\mathbf{Y}_{c,ii} \xrightarrow{s \rightarrow 0} \sqrt{\frac{\mathbf{G}_{ii}}{\mathbf{R}_{ii}}} \quad (15)$$

$$\mathbf{H}_{ii} \xrightarrow{s \rightarrow 0} e^{-\sqrt{\mathbf{R}_{ii}\mathbf{G}_{ii}}l}. \quad (16)$$

In the present work, it is proposed to choose the conductance value such that the voltage in a trapped charge simulation will discharge with a predefined time constant, T , for instance 1 s. This gives

$$\mathbf{G}_{ii} = \frac{\mathbf{C}_{ii}}{T}. \quad (17)$$

This value gives for all diagonal terms $\mathbf{G}_{ii} + s\mathbf{C}_{ii}$ in (14) a zero (root)

$$s_1 = -\frac{1}{T}. \quad (18)$$

A zero appears for each diagonal term $\mathbf{R}_{ii} + s\mathbf{L}_{ii}$ in (15) at

$$s_2 = -\frac{\mathbf{R}_{ii}}{\mathbf{L}_{ii}}. \quad (19)$$

In order to capture the modified low-frequency behavior, the lower band limit for the rational fitting is taken as

$$\omega_{low} = 0.1 \cdot \min(s_1, s_2). \quad (20)$$

In the case of coaxial cables, the core conductor does not have a direct coupling to ground and so adding a conductance to the diagonal elements of \mathbf{G} is unphysical. Therefore, the conductance specification and the zeros calculation (s_1, s_2) is based on the cable loop parameters [21] rather than phase parameters.

B. High-Frequency Passivity Violations

Asymptotic passivity for \mathbf{Y}_c is enforced by replacing (5) and (6) with

$$\text{tr}(\mathbf{Y}_c) - \text{tr}(\mathbf{Y}_c^\infty) \cong \sum_{m=1}^N \frac{r_m}{s - a_m} \quad (21)$$

$$\mathbf{Y}_c - \mathbf{Y}_c^\infty \cong \sum_{m=1}^N \frac{\mathbf{R}_m}{s - a_m}. \quad (22)$$

Thus, the constant term \mathbf{D} is taken as \mathbf{Y}_c^∞ , thereby ensuring that the rational model for \mathbf{Y}_c is positive real at infinite frequency. In the practical implementation, we use an approximate

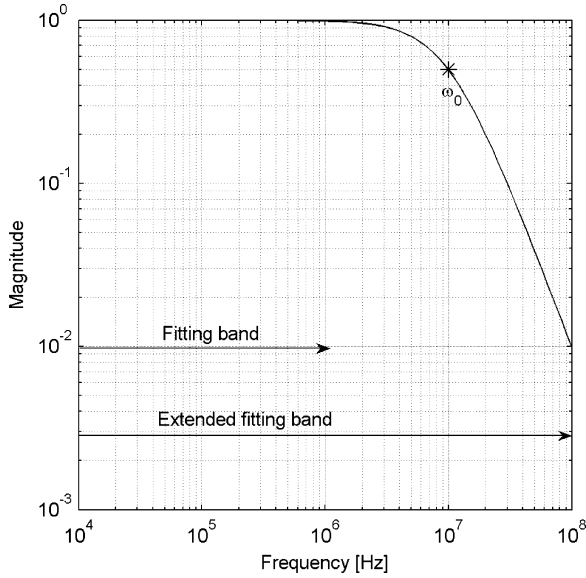


Fig. 1. Filter response, magnitude ($\omega_0 = 2\pi \cdot 1\text{E}7$ Hz).

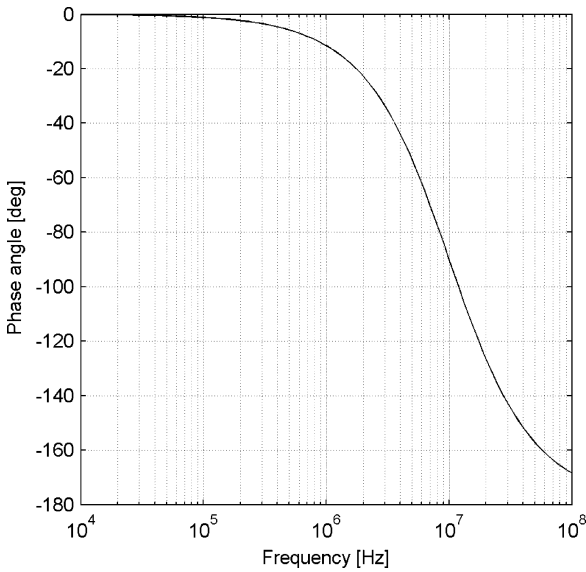


Fig. 2. Filter response, phase angle.

```

Dcorr = 0
for  $k=1:N_s$ 
     $\mathbf{Y}_H(s_k) + \mathbf{D}_{corr} \rightarrow \mathbf{T}\mathbf{A}_{pos}\mathbf{T}^{-1} + \mathbf{T}\mathbf{A}_{neg}\mathbf{T}^{-1}$ 
     $\mathbf{D}_{corr} := \mathbf{D}_{corr} - \alpha \cdot \text{Re}\{\mathbf{T}\mathbf{A}_{neg}\mathbf{T}^{-1}\}$ 
end

```

Fig. 3. Pseudo code for calculating correction term.

value \mathbf{Y}_c^∞ , taken as $\text{Re}\{\mathbf{Y}_c\}$ with \mathbf{Y}_c evaluated at a high-frequency point above the upper band limit.

The propagation function \mathbf{H} and its modes are multiplied by a low-pass filter response. The cutoff frequency ω_0 is placed one decade above the upper frequency limit that is to be used in the fitting process. The fitting band is extended one decade beyond

ω_0 in order to include the modified behavior of \mathbf{H} . As low-pass filter, we propose the second-order filter (23) with $\zeta = 1.01$, see Figs. 1 and 2. It is seen that within the original fitting band, the impact of the filter is small. (This filter is slightly overdamped as usage of critical damping $\zeta = 1$ would give a double pole, thereby causing difficulties for the fitting process). This choice of filter response is somewhat arbitrary and better alternatives may exist

$$g(s) = \frac{1}{1 + 2\zeta \frac{s}{\omega_0} + \left(\frac{s}{\omega_0}\right)^2}. \quad (23)$$

V. REMOVAL OF REMAINING PASSIVITY VIOLATIONS

The presence of any remaining (small) passivity violations is removed by adding a correction term to the model. For that purpose, a rational model is connected externally to the transmission line ports. Using the Simplistic Approach [14, Section VII], [25], a correction matrix \mathbf{D}_{corr} is established by sweeping \mathbf{Y}_H in (10) over a band of frequency samples. At each frequency sample, \mathbf{Y}_H is factored into two modal decompositions that respectively contain the positive and negative eigenvalues.

$$\mathbf{Y}_H = \mathbf{T}\mathbf{A}\mathbf{T}^{-1} = \mathbf{T}\mathbf{A}_{pos}\mathbf{T}^{-1} + \mathbf{T}\mathbf{A}_{neg}\mathbf{T}^{-1}. \quad (24)$$

By taking the negated value of the second term in (24) as a correction term, one can ensure that all eigenvalues of \mathbf{Y}_H are positive (or zero), at that frequency. Embedding this procedure within a frequency sweep makes all eigenvalues non-negative at all frequencies in the sweep. The procedure is shown in Fig. 3. In this implementation, the (small) imaginary part of \mathbf{D}_{corr} is discarded in order to obtain a real, symmetrical \mathbf{D}_{corr} . As a result, the correction step may at a given frequency have to be repeated a few times. The number of iterations is kept low by using a factor α in Fig. 3 slightly greater than unity. In this paper, we used $\alpha = 1.1$.

The correction \mathbf{D}_{corr} is in the form of a nodal conductance matrix that gives an instantaneous coupling between all terminals. The correction can be limited in bandwidth by multiplying with a suitable band-pass filter. If the passivity violations are located between frequencies $\{\omega_1, \omega_2\}$, it is proposed to use a correction

$$\mathbf{P}(s) = \mathbf{D}_{corr} \frac{-1.01 \cdot (-10\omega_2)s}{(s - (-0.1\omega_1))(s - (-10\omega_2))}. \quad (25)$$

In (25), the two poles are respectively placed at one decade below and above ω_1 and ω_2 , thus ensuring that the imaginary part of the band-pass filter is negligible between ω_1 and ω_2 . The factor 1.01 ensures that the real part of the bandpass filter is greater than unity at the boundaries ω_1 and ω_2 .

It is observed that (25) can be expanded into a sum of pole-residue terms (26). The inclusion of (26) in an EMTP type simulation environment is a well established procedure, being done via an equivalent electrical network [23], or via recursive convolution [1] and a companion network—see Fig. 4.

$$\mathbf{P}(s) = \frac{\mathbf{R}_1}{s - a_1} + \frac{\mathbf{R}_2}{s - a_2}. \quad (26)$$

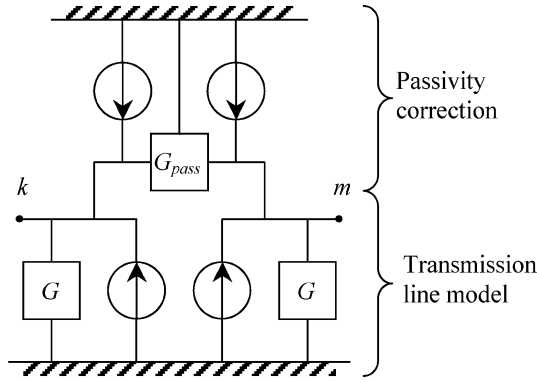


Fig. 4. Including passivity correction in EMT simulation.

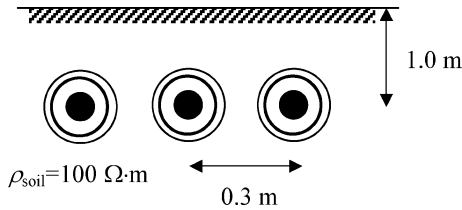


Fig. 5. Cable configuration. Cable length: 1000 m.

TABLE I
SC CABLE DATA

Item	Property
Core	OD=39 mm, $\rho=3.365E-8 \Omega\text{m}$
Insulation	$t=18.25$ mm, $\epsilon_r=2.85$
Sheath	$t=0.22$ mm, $\rho=1.718E-8 \Omega\text{m}$
Jacket	$t=4.53$ mm, $\epsilon_r=2.51$

VI. EXAMPLE: THREE SINGLE CORE COAXIAL CABLES

A. Cable Geometry

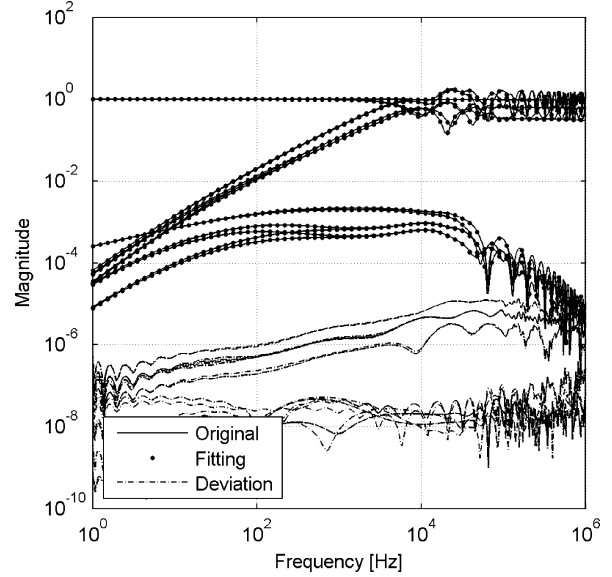
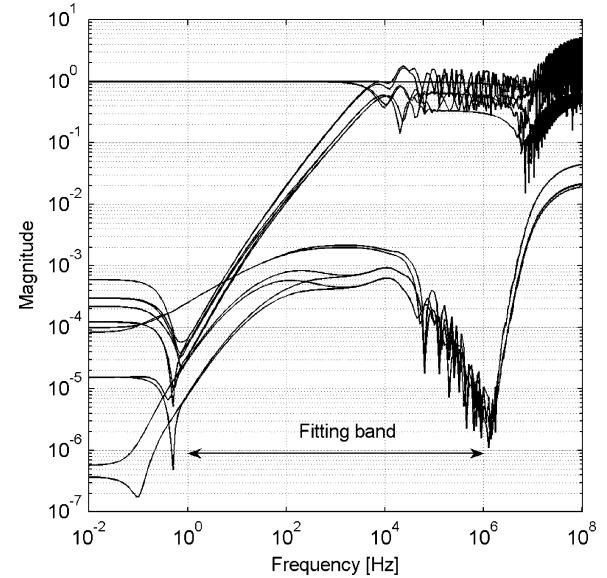
Fig. 5 shows three 145-kV single-core coaxial cables with data given in Table I.

B. Result With Original Modeling Procedure

The six modes of \mathbf{H} were lumped into four modes that were each fitted using 20 poles in the band 1 Hz–1 MHz, followed by a final fitting of \mathbf{H} in the phase domain. Fig. 6 shows the resulting fitting of the elements of \mathbf{H} . Clearly, a very accurate result has been obtained within the fitting band. Fig. 7 shows the same result over a wider band, 0.01 Hz – 100 MHz. It is seen that the behavior of \mathbf{H} changes abruptly when moving out of the fitting band.

From the rational approximation of \mathbf{H} and \mathbf{Y}_c , the nodal admittance matrix \mathbf{Y}_n was calculated using (11)–(13). The corresponding plot of eigenvalues of \mathbf{Y}_H in Fig. 8 shows large passivity violations (negative eigenvalues) in the low-frequency and the high-frequency region.

The effect of the passivity violations on stability is demonstrated for the step voltage excitation example in Fig. 9. Fig. 10 shows the simulated (PSCAD) far end response on terminal 7. The response is seen to become unstable after about 25 μs .

Fig. 6. Rational approximation of \mathbf{H} .Fig. 7. Wideband behavior of fitted \mathbf{H} .

C. Result With Prevention of Out-of-Band Passivity Violations

In order to overcome the instability problem in Fig. 10, the mitigating techniques in Section IV are applied.

- 1) A shunt conductance term is added to remove low-frequency passivity violations. The conductance is chosen so as to give a time constant of 1 sec for the discharge of the core-sheath and sheath-ground loop capacitances (17). The lower limit of the fitting band is extended downwards by (20).
- 2) Asymptotic passivity of \mathbf{Y}_c is enforced by (21)–(22).
- 3) The elements of \mathbf{H} are multiplied with a second-order low-pass filter with $\omega_0 = 2\pi \cdot 1 E7$ rad/s, $\zeta = 1.01$. The upper limit of the fitting band is extended 1 decade above ω_0 , to 1 E8 Hz.

Fig. 11 shows that adding a shunt conductance to the diagonal elements of \mathbf{Y} leads to a controlled (constant) behavior of \mathbf{Y}_c

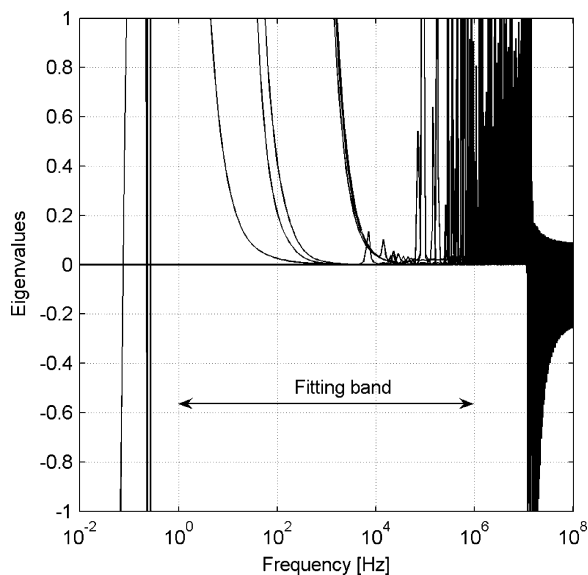


Fig. 8. Eigenvalues of $Y_H(s)$.

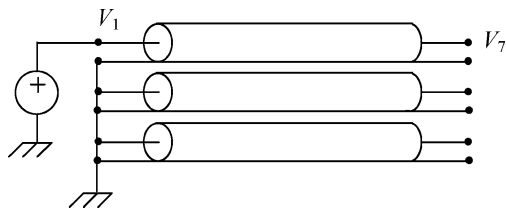


Fig. 9. Step voltage excitation.

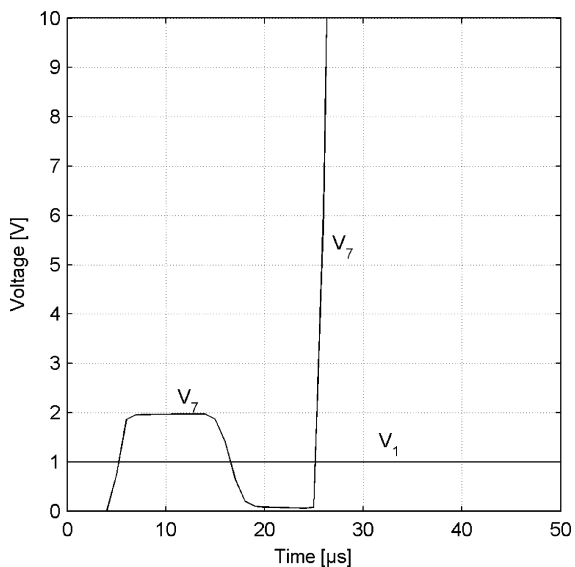


Fig. 10. Open circuit response (unstable). $\Delta t = 1E - 6$ sec.

at low frequencies. This low-frequency behavior is seen to be captured by the rational model.

The effect on the fitted H is shown in Fig. 12. Compared to the previous result (Fig. 7), the elements of H now approach high-frequency values that are much smaller than unity.

Fig. 13 shows the eigenvalues of Y_H . Compared to the previous result (Fig. 8), all eigenvalues are now positive in the full

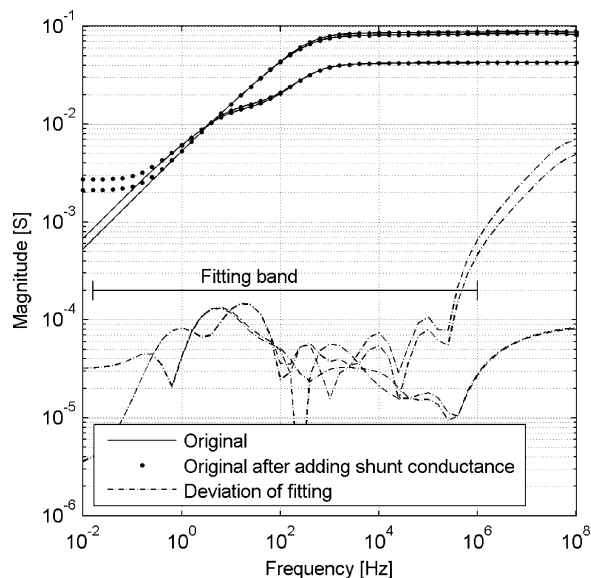


Fig. 11. Wideband behavior of Y_c . (Diagonal elements, 10th order).

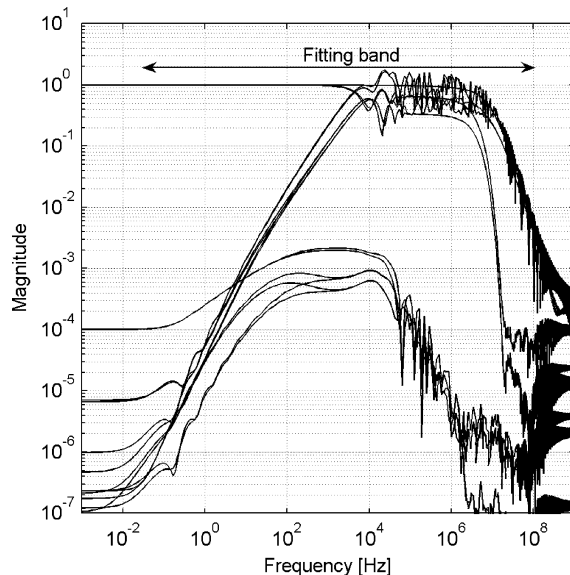


Fig. 12. Wideband behavior of fitted H .

band, except for some very small violations between 1 Hz and 10 kHz. The small violations are better observed in the expanded plot in Fig. 16 (solid traces).

Fig. 14 shows a simulation of the step response for the case in Fig. 9. A stable simulation is achieved, contrary to the previous result without passivity handling (Fig. 10). Fig. 15 shows the far end voltage when the cable is disconnected shortly after energization. The trapped voltage is seen to decay nearly exponentially with a time constant equal to the specified one (1 s).

D. Result With Removal of Remaining Passivity Violations

In Fig. 13, some very small passivity violations were found to be present. Using the approach in Section V, these violations are removed by adding a correction term externally to the transmission line terminals. The correction term by (26) is included in the PSCAD simulation via a user-written subroutine [22].

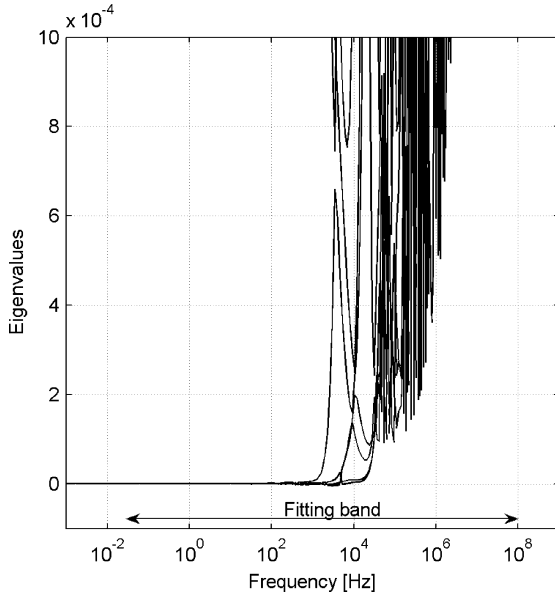
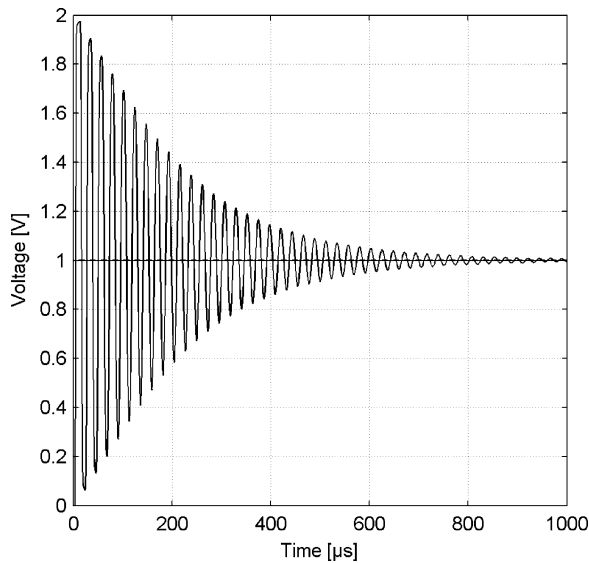
Fig. 13. Eigenvalues of $\mathbf{Y}_H(s)$.Fig. 14. Open circuit response (stable). $\Delta t = 1E - 6$ sec.

Fig. 16 shows the effect on the eigenvalues of \mathbf{Y}_H . It is seen that the eigenvalues become modified in a local frequency band, making them positive. Since the correction term is very small, the effect on a transient simulation is also small. Fig. 17 shows the far end cable voltage for the step voltage excitation in Fig. 9. The deviation from the result without passivity correction (Fig. 14) is smaller than $3E - 4$ in peak value. On the other hand, the effect on a trapped charge voltage simulation is substantial, see Fig. 18. The correction term effectively increases the shunt conductance at frequencies above dc, leading to an initially faster discharge of the cable.

E. Transient Sheath Overvoltage

As a validation test we compare a simulated voltage response with that by the Fourier transform. One cable sheath is subjected to a step voltage excitation (V_2), and the resulting far end voltage

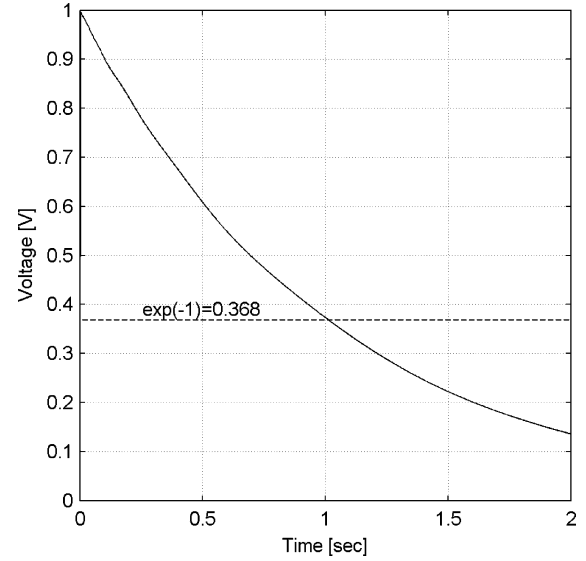


Fig. 15. Trapped charge simulation.

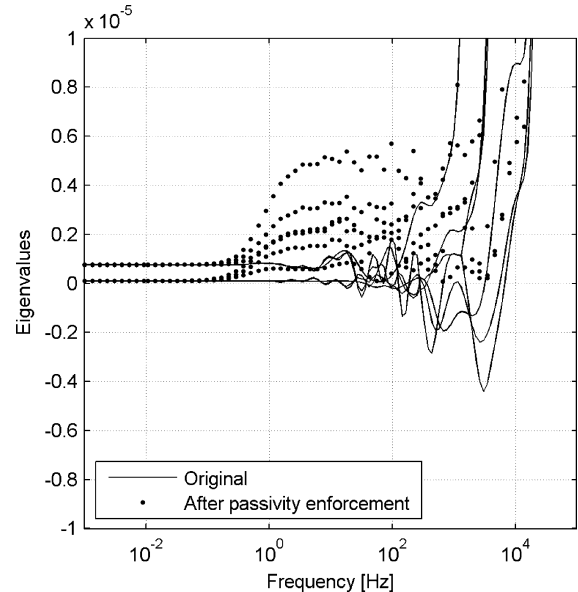


Fig. 16. Removal of remaining passivity violations.

on the same sheath (V_8) is to be calculated, see Fig. 19. Figs. 20 and 21 show the simulated sheath voltage by PSCAD using the passivated ULM model ($\Delta t = 1E - 7$ s). In the same plot is also shown the result by the inverse Fourier transform using the procedure in [15] with a 1-MHz upper frequency limit. Clearly, a very close agreement has been achieved.

VII. DISCUSSION

The problem of unstable simulations due to passivity violations is usually a problem with short transmission lines. Here, the elements of the propagation function are insignificantly attenuated at the upper frequency limit specified by the user of the EMT program. Usage of a high-order fitting can then easily result in high-frequency out-of-band passivity violations, and unstable simulations often result with a small time step. Introducing an artificial attenuation at high frequencies for the fitting

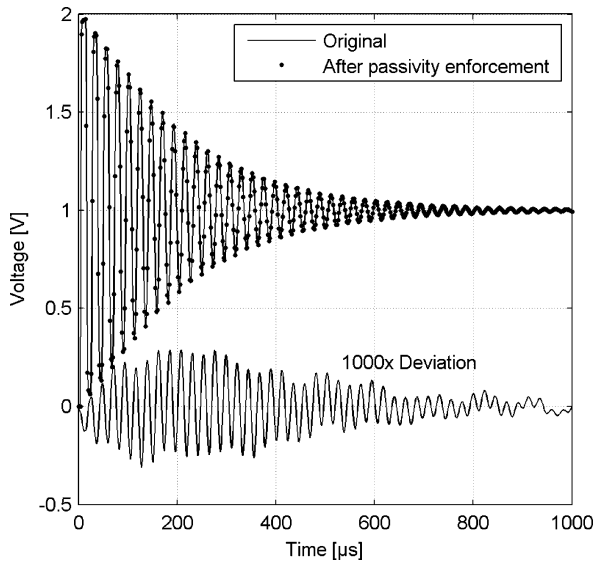


Fig. 17. Effect of correction term on transient voltage.

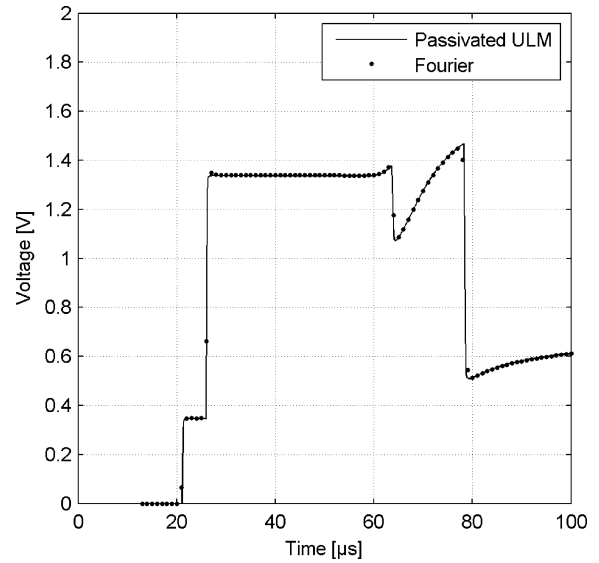


Fig. 20. Simulated sheath voltage (initial response).

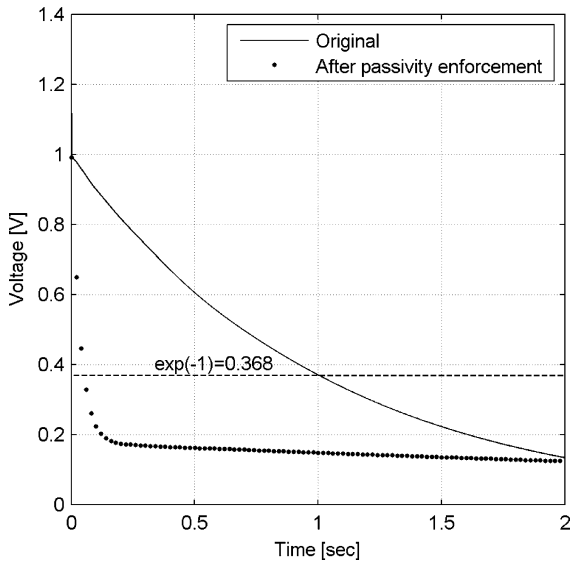


Fig. 18. Effect of correction term on trapped voltage.

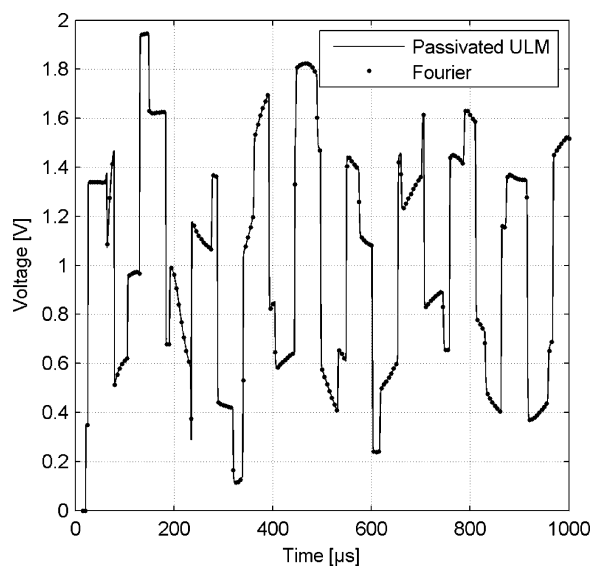


Fig. 21. Simulated sheath voltage (expanded view).

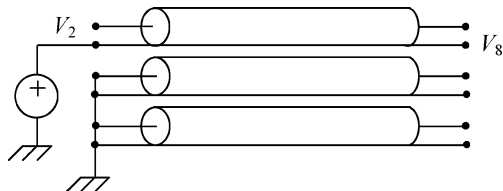


Fig. 19. Sheath voltage excitation.

of \mathbf{H} was shown to be an efficient way of removing high-frequency passivity violations. In principle, one can achieve a similar result by simply extending the fitting range to a very high frequency. However, in the case of short line stubs, the upper frequency limit could become very high, causing problems in the evaluation of the series impedance. Also, increasing the upper frequency tends to increase the number of delay groups in ULM, thereby reducing the computational efficiency of the model. In the case of long lines with a significant attenuation at the upper

frequency limit, it is probably wise to not introduce the low-pass filter since the accuracy within the fitting band will for a given fitting order decrease. It is remarked that high-frequency passivity violations is not an issue with line models that are based on modes and asymptotic fitting [2] as that fitting approach ensures a controlled behavior for the asymptotic high-frequency value of \mathbf{H} .

A controlled behavior for the line model at near dc conditions is achieved by introducing an artificial conductance, thereby giving a nonzero magnitude for \mathbf{Y}_c at dc. For this to work in practice, one has to ensure that the fitting band is extended sufficiently low in frequency to capture the modified low-frequency (constant) behavior, e.g., by (20). Also, the fitting order must be sufficiently high so that the low-frequency behavior is included in the model with sufficient accuracy.

It was shown that the above measures prevent the occurrence of large out-of-band passivity violations. Small violations may

still remain within the frequency band, but their presence can be removed by introducing an external correction term as shown in Section V. Since this term leads to a direct connection between the two line ends, the delay properties of the line becomes corrupted by a small amount. For the response in Fig. 20, the sheath voltage prior to wave arrival ($21 \mu\text{s}$) is smaller than $3E - 5$, thus being negligible. A more practical disadvantage is that a trapped charge may discharge too fast, see Fig. 18.

An alternative to the Simplistic Approach (Section V), for removing in-band passivity violations, is to iteratively perturb the model parameters. A recent paper [26] describes a procedure for achieving this, showing results for a single conductor line. It is remarked that any approach based on perturbation may diverge whereas the Simplistic Approach will never diverge. On the other hand, using perturbation can possibly lead to smaller corrections.

VIII. CONCLUSIONS

This paper has shown that unstable simulations can occur with the Universal Line Model due to out-of-band passivity violations at low and high frequencies. The problem is overcome by the following steps.

- 1) Low-frequency violations are prevented from occurring by adding a shunt conductance to the diagonal elements of the shunt admittance, \mathbf{Y} . The value of the conductance is chosen based on a required time constant for trapped voltage decay, and the lower limit of the fitting band is extended towards lower frequencies in order to capture the modified low-frequency behavior.
- 2) High-frequency violations are prevented from occurring by multiplying the propagation function \mathbf{H} with a low-pass filter response. The upper limit of the fitting band is extended towards higher frequencies to include the modified high-frequency behavior in the fitting process. In addition, asymptotic high-frequency passivity is enforced for the characteristic admittance, \mathbf{Y}_c .
- 3) Any remaining passivity violations are removed by introducing a low order correction term that connects between the terminals of the line.

REFERENCES

- [1] A. Semlyen and A. Dabuleanu, "Fast and accurate switching transient calculations on transmission lines with ground return using recursive convolutions," *IEEE Trans. Power App. Syst.*, vol. 94, no. 2, pp. 561–575, Mar./Apr. 1975.
- [2] J. R. Marti, "Accurate modelling of frequency-dependent transmission lines in electromagnetic transient simulations," *IEEE Trans. Power App. Syst.*, vol. 101, no. 1, pp. 147–157, Jan. 1982.
- [3] G. Angelidis and A. Semlyen, "Direct phase-domain calculation of transmission line transients using two-sided recursions," *IEEE Trans. Power Del.*, vol. 10, no. 2, pp. 941–949, Apr. 1995.
- [4] T. Noda, N. Nagaoka, and A. Ametani, "Phase domain modeling of frequency-dependent transmission lines by means of an ARMA model," *IEEE Trans. Power Del.*, vol. 11, no. 1, pp. 401–411, Jan. 1996.
- [5] H. V. Nguyen, H. W. Dommel, and J. R. Marti, "Direct phase-domain modelling of frequency-dependent overhead transmission lines," *IEEE Trans. Power Del.*, vol. 12, no. 3, pp. 1335–1342, Jul. 1997.
- [6] B. Gustavsen and A. Semlyen, "Combined phase and modal domain calculation of transmission line transients based on vector fitting," *IEEE Trans. Power Del.*, vol. 13, no. 2, pp. 596–604, Apr. 1998.

- [7] B. Gustavsen and A. Semlyen, "Calculation of transmission line transients using polar decomposition," *IEEE Trans. Power Del.*, vol. 13, no. 3, pp. 855–862, Jul. 1998.
- [8] A. Morched, B. Gustavsen, and M. Tartibi, "A universal model for accurate calculation of electromagnetic transients on overhead lines and underground cables," *IEEE Trans. Power Del.*, vol. 14, no. 3, pp. 1032–1038, Jul. 1999.
- [9] B. Gustavsen, G. Irwin, R. Mangelrød, D. Brandt, and K. Kent, "Transmission line models for the simulation of interaction phenomena between parallel AC and DC overhead lines," in *Proc. Int. Conf. Power System Transients (IPST)*, Jun. 20–24, 1999, pp. 61–67.
- [10] B. Gustavsen and J. Nordstrom, "Pole identification for the universal line model based on trace fitting," *IEEE Trans. Power Del.*, vol. 23, no. 1, pp. 472–479, Jan. 2008.
- [11] [Online]. Available: <http://pscad.com/>.
- [12] B. Gustavsen and A. Semlyen, "Rational approximation of frequency domain responses by vector fitting," *IEEE Trans. Power Del.*, vol. 14, no. 3, pp. 1052–1061, Jul. 1999.
- [13] P. Triverio, S. Grivet-Talocia, M. S. Nakhla, F. G. Canavero, and R. Achar, "Stability, causality, and passivity in electrical interconnect models," *IEEE Trans. Adv. Packag.*, vol. 30, no. 4, pp. 795–808, Nov. 2007.
- [14] B. Gustavsen and A. Semlyen, "Enforcing passivity for admittance matrices approximated by rational functions," *IEEE Trans. Power Syst.*, vol. 16, no. 1, pp. 97–104, Feb. 2001.
- [15] B. Gustavsen, "Validation of frequency dependent transmission line models," *IEEE Trans. Power Del.*, vol. 20, no. 2, pp. 925–933, Apr. 2005.
- [16] E. Ghad, C. Chen, M. Nakhla, and R. Achar, "Passivity verification in delay-based macromodels of electrical interconnects," *IEEE Trans. Circuits Syst. I*, vol. 52, no. 10, pp. 2173–2187, Oct. 2005.
- [17] J. R. Marti, "The Problem of Frequency Dependence in Transmission Line Modelling," Ph.D. dissertation, University of British Columbia, BC, Canada, 1981.
- [18] EMTDC User's Guide. Winnipeg, MB, Canada, The Manitoba HVDC Research Centre, 2003.
- [19] S. Grivet-Talocia and F. Canavero, "DC-compliant macromodels based on the method of characteristics for frequency-dependent transmission lines," in *Proc. Electronics Systemintegration Technology Conf.*, Dresden, Germany, Sep. 5–7, 2006, pp. 56–61.
- [20] A. B. Fernandes, W. L. A. Neves, E. Costa, and M. N. Cavalcanti, "Transmission line shunt conductance from measurements," *IEEE Trans. Power Del.*, vol. 19, no. 2, pp. 722–728, Apr. 2004.
- [21] L. M. Wedephol and D. J. Wilcox, "Transient analysis of underground power-transmission systems. System-model and wave-propagation characteristics," *Proc. Inst. Elect. Eng.*, vol. 120, no. 2, pp. 253–260, Feb. 1973.
- [22] B. Gustavsen and O. Mo, "Interfacing convolution based linear models to an electromagnetic transients program," in *Proc. Int. Conf. Power Systems Transients*, Lyon, France, Jun. 4–7, 2007, p. 6.
- [23] A. Morched, J. Ottevangers, and L. Marti, "Multi-port frequency dependent network equivalents for the EMTP," *IEEE Trans. Power Del.*, vol. 8, no. 3, pp. 1402–1412, Jul. 1993.
- [24] S. Grivet-Talocia, "Passivity enforcement via perturbation of Hamiltonian matrices," *IEEE Trans. Circuits Syst. I*, vol. 51, no. 9, pp. 1755–1769, Sep. 2004.
- [25] B. Gustavsen, "Robust passivity enforcement for frequency dependent transmission line models," in *Proc. 11th IEEE Workshop on Signal Propagation on Interconnects*, Ruta di Camogli (Genova), Italy, May 13–16, 2007, pp. 169–172.
- [26] A. Chinaea and S. Grivet-Talocia, "A passivity enforcement scheme for delay-based transmission line macromodels," *IEEE Microw. Wireless Compon. Lett.*, vol. 17, pp. 562–564, 2007.

Bjørn Gustavsen (M'94–SM'03) was born in Harstad, Norway, in 1965. He received the M.Sc. and Dr.Eng. degrees from the Norwegian Institute of Technology (NTH), Trondheim, Norway, in 1989 and 1993, respectively.

Since 1994, he has been with SINTEF Energy Research. He spent 1996 as a Visiting Researcher at the University of Toronto, Toronto, ON, Canada, and the summer of 1998 at the Manitoba HVDC Research Centre, Winnipeg, MB, Canada. He was a Marie Curie Fellow at the University of Stuttgart, Germany, from August 2001 to August 2002. His interests include simulation of electromagnetic transients and modeling of frequency dependent effects.